Chinese Journal of Aeronautics, (2015), 28(6): 1583–1592

Chinese Society of Aeronautics and Astronautics
& Beihang University

Chinese Journal of Aeronautics

cja@buaa.edu.cn
www.sciencedirect.com

Experimental and computational investigation of adsorption performance of TC-5A and PSA-5A for manned spacecraft

Liu Meng [a], Yang Dongsheng [a], Pang Liping [a,*], Yu Qingni [b], Huang Yong [a]

[a] *School of Aeronautic Science and Engineering, Beihang University, Beijing 100191, China*
[b] *National Key Laboratory of Human Factors Engineering, China Astronaut Research and Training Center, Beijing 100094, China*

Received 9 April 2015; revised 1 July 2015; accepted 21 July 2015
Available online 29 August 2015

KEYWORDS

CO_2 adsorption;
Dynamic simulation;
Experimental analysis;
Manned spacecraft;
Molecular sieve

Abstract Two kinds of molecular sieve materials, TC-5A and PSA-5A, were produced to satisfy with special requirement of manned space flight. Their CO_2 adsorption performances were investigated and compared through two experiments, the thermo gravimetric analysis (TGA) experiment and packed bed column experiment. Besides, some kinetic equations were compared according to the TGA experimental data, and their errors were analyzed. Finally, the classic linear driving force (LDF) model is improved to the new Avrami's model, and two models are analyzed based on the packed bed data. The TGA data shows that the CO_2 loading has an approximately linear relationship with the CO_2 concentration, and the best fit adsorption temperature range is from 283 to 303 K. The packed bed column results show that water vapor in air can affect the CO_2 adsorption performance badly. The new Avrami's model is proved more suitable to reflect the complex adsorption mechanism for two molecular sieves. The materials are proved having much better adsorption capacity than the other adsorbents with room temperature and low CO_2 concentration ($\leqslant$1.0% in volume), and they can meet the aerospace requirements. This work will benefit the optimal design and simulation of the air revitalization (AR) system for Chinese manned spacecraft.

1. Introduction

CO_2 adsorption and separation technology, such as the solution absorption, membrane separation technique, cryogenic techniques and adsorption over solid sorbents,[1,2] have been explored and widely employed in industrial field. Some mature technologies are even applied to the manned spacecraft, like the Apollo, Skylab and International Space Station (ISS).

* Corresponding author. Tel.: +86 010 82313186.
E-mail addresses: liumeng@buaa.edu.cn (M. Liu), xingyewuhen@163.com (D. Yang), pangliping@buaa.edu.cn (L. Pang), yuqingni@139.com (Q. Yu), huangy@buaa.edu.cn (Y. Huang).
Peer review under responsibility of Editorial Committee of CJA.

Production and hosting by Elsevier

http://dx.doi.org/10.1016/j.cja.2015.08.003

Short-duration manned spacecraft, such as Mercury, Apollo and Space Shuttle of America, "Shenzhou" series of China, generally adopts hydroxide adsorbent in non-regenerative way.[3] But a regenerative environmental control system (ECS) needs to be developed in order to keep cabin's atmospheric quality control for its complex long-term space exploration missions.[4,5] At present, the integrated air revitalization (AR) subsystem has low adsorption efficiency in regenerative process,[6] and the high-efficiency adsorbent needs to be developed for the closed-loop AR subsystem to satisfy the requirement of long-duration manned spacecraft.[5,7–9] As the adsorption performance of adsorbents determines the system's character, such as volume, mass, cost of power, cycle duration, service life and the possible pollution,[3,6,10,11] the adsorption performance of adsorbent should be investigated in great detail.

In the past few years, various adsorbents have been developed and applied in separation processes in industry. The materials include Zeolite 3A and 4A, carbon molecular sieves (CMS), natural clinoptilolite membrane, molecular basket sorbent (MBS), hollow polymeric fibers, oxide octahedral molecular sieve (OMS-2) catalysts, etc.[12–19] Some of them even considered the influencing factors, such as initial concentrations, temperatures, and particle sizes. According to the four consecutive elementary steps of adsorption process mechanism, different equations for particles and the fixed bed have been proposed, including the Pseudo-first order equation, Elovich's equation, Pseudo-second order rate equation, Avrami's kinetic equation and Fractional order kinetic equation.[20–28] Besides, the mass transfer mechanism in a fixed bed column can be described by modeling and simulation so as to predict the adsorbent performance under any condition.[1,6,29–34]

In this paper, two molecular sieves materials, TC-5A and PSA-5A, are investigated regarding their adsorption performance for the future manned space application in China. The CO_2 adsorption performance experiments for particles were tested by the TGA experiment, and the best fit kinetic equation is proposed based on the experimental results. In addition, the influences of some factors, such as initial concentration, temperature and relative humidity (RH), on the CO_2 adsorption are also studied in the packed column experiments. Finally, the improved mathematical model for two adsorption materials in the fixed bed is established by using an Avrami's equation.

2. TC-5A and PSA-5A molecular sieve for manned spacecraft

The CO_2 adsorption performance of molecular sieve determines the efficiency of AR subsystem,[6] hence the development of materials is one of the critical factors for the manned technologies. For this purpose, two kinds of molecular sieves products, PSA-5A and TC-5A, were made for the future manned space application in China. The producing process has been adjusted a lot to come up with the requirement of the manned environment. Fig. 1 shows the formation images of TC-5A and PSA-5A, two molecular sieves used basically identical raw materials, but shaped different average particle sizes. The physical parameters are shown in Table 1.

The standard tests show that their rigidity, thermal stability and mean diameter can satisfy special requirements of AR subsystem. Their thermal vacuum desorption and revitalization in packed bed column are easy to carry out under the condition of 423–573 K and low pressure vacuum (< 100 Pa).

(a) TC-5A molecular sieve

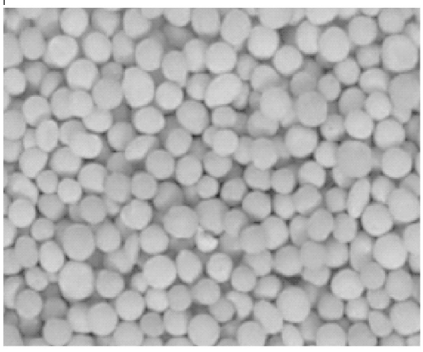

(b) PSA-5A molecular sieve

Fig. 1 Two molecular sieve materials.

Table 1 Physical parameters of molecular sieves.

Parameter	TC-5A	PSA-5A
Porosity ε_b (%)	0.500	0.454
Density ρ_p (kg/m^3)	1223	1223
Specific surface area A_s (m^2/g)	552	647
Mean diameter D_p (mm)	2.00	0.75
Pore volume V (10^{-6} m^3/g)	0.27	0.40

3. TGA experiments and adsorption kinetic equations

In order to investigate the CO_2 adsorption performance of two molecular sieves and to build the corresponding kinetic equations, the TGA experiments were carried out at different concentration and temperature conditions.

The CO_2 adsorption of molecular sieve is a physical process and its equilibrium adsorption capacity is greatly influenced by the adsorption temperature and the CO_2 concentration. In the following experiments, the isothermal adsorption process would be used to obtain the CO_2 adsorption performance. In the experiments, the temperature range was 293–323 K and the CO_2 concentration was less than 1.0% in volume.

3.1. Experiments setup and procedure

Schematic diagram and apparatus photo of TGA experiment are shown in Figs. 2 and 3, respectively. The experimental design steps are as follows:

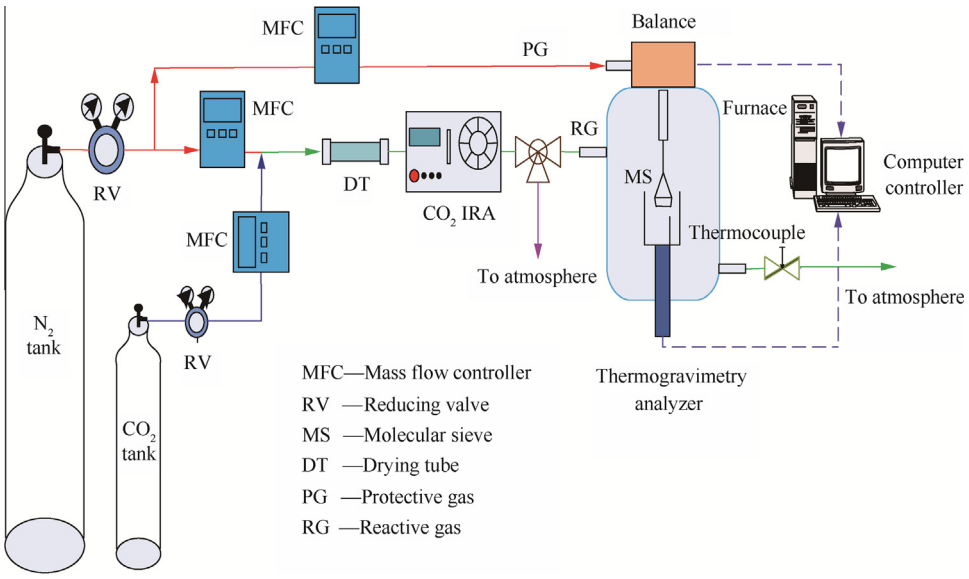

Fig. 2 Schematic diagram of TGA experiment.

Fig. 3 Apparatuses photo of TGA experiment.

(1) Adsorption temperature of TC-5A and PSA-5A, $T_{TC\text{-}5A}$ and $T_{PSA\text{-}5A}$, maintaining at 298 K or 323 K.
(2) The volumetric flow rate of feed air is 100 mL/min. The feed air is produced by mixing pure N_2 and CO_2 at a certain volume ratio. In our experiments, the CO_2 volume concentration of feed air, C_{CO_2}, is maintained at 0.5%, 0.7% and 1.0% separately, by the mass flow-meters.
(3) The CO_2 concentration in feed air is monitored by infrared red analyzer (IRA).
(4) A drying tube with silicone 13X is added to the N_2 pipeline to remove water vapor in advance.
(5) All desorption temperatures keep at 533 K with pure N_2 as protective gas at 100 mL/min flow rate.

The experimental apparatus are shown in Table 2.

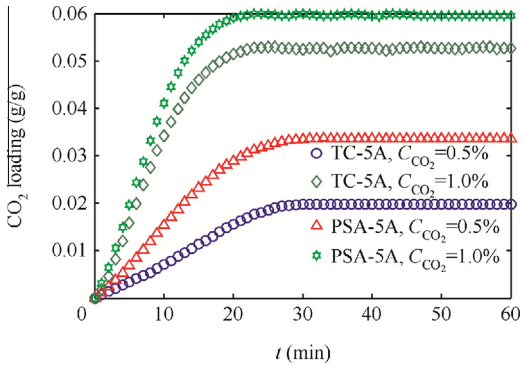

Fig. 4 Adsorption curves of two materials with different concentrations at 298 K.

3.2. Experimental results and analysis

3.2.1. Concentration factor

CO_2 equilibrium adsorption capacity of molecular sieve has a functional relationship with initial CO_2 concentration at a given temperature. Fig. 4 shows adsorption curves varying with time t for the two molecular sieve materials when C_{CO_2} = 0.5% and C_{CO_2} = 1.0% at 298 K, seperately. Some results can be summarized from Fig. 4:

Table 2 Experimental apparatus.

No.	Apparatus	Accuracy	Manufacturer
1	TGA	±0.1 (μg)	Mettler Toledo
2	Low-temperature thermostat bath	±0.01 (K)	Ningbo Tianheng Instrument Factory
3	Infrared gas analyzer	±0.01 (%)	Beijing BAIF-Maihak Analytical Instrument Co., Ltd
4	Mass flow controller	±0.01 (mL)	ALICAT of America

(1) It takes about 45 min to reach equilibrium for TC-5A and the adsorption capacity is 0.019744 g/g (gas/adsorbent) when C_{CO_2} = 0.5% and $T_{TC\text{-}5A}$ = 298 K. While the TC-5A adsorption time decreases to 35 min when C_{CO_2} = 1.0%, and the adsorption capacity becomes 0.05274 g/g. In comparison, the PSA-5A adsorption time is about 32 min when C_{CO_2} = 1.0%, and its adsorption capacity reaches 0.05993 g/g.
(2) Both molecular sieve materials are largely affected by the inlet CO_2 concentration. Yet the adsorption capacity of PSA-5A shows larger than the one of TC-5A.
(3) The adsorption capacity of two molecular sieves is 0.02–0.06 g/g when C_{CO_2} = 0.5% to 1.0% at 298 K. In our subsequent experiment, the adsorption capacity of TC-5A is 0.055 g/g when C_{CO_2} = 0.7% at 290 K.

Compared with the industrial adsorbent with the CO_2 capability of 0.01–0.03 g/g with low concentration, the experimental results demonstrate that the TC-5A and PSA-5A have superior CO_2 uptake performance and are capable of satisfying the adsorption requirements of the manned spacecraft at low CO_2 concentration and room temperature.

3.2.2. Temperature factor

Temperature is another key factor that impacts on the interaction force of physical adsorption. We compare the CO_2 uptake curves of TC-5A and PSA-5A at 298 and 323 K, respectively, when C_{CO_2} = 0.75%, as shown in Fig. 5. When the feed air temperature rises to 323 K, the CO_2 uptake of TC-5A and PSA-5A inconceivably decreases by 80%. The adsorption capacity of TC-5A decreases from 0.0453 to 0.0132 g/g and PSA-5A decreases from 0.0373 to 0.0115 g/g. Their adsorption time only sustains 20 min more or less. The curves in Fig. 5 also show that temperature rising can reduce the adsorption capacity gap when both CO_2 loading decreases badly.

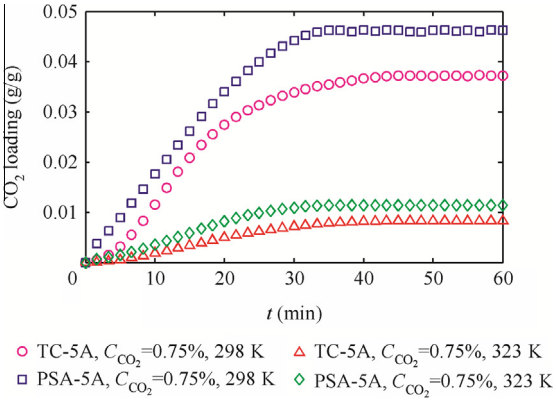

Fig. 5 Comparison of CO_2 uptake curves between TC-5A and PSA-5A at different temperatures.

3.3. Adsorption kinetics equation

It is necessary to establish one appropriate kinetic equation to evaluate its adsorption capacity and comprehend the adsorption process. Many kinetic models have been represented to describe the solid–liquid phase adsorption, but few models depict the solid–gas process due to its complexity. Therefore, in this section, some kinetic models will be discussed in order to correctly reflect the solid–gas adsorption process for TC-5A and PSA-5A. Five typical kinetic equations will be analyzed as listed in Table 3.

In Table 3, $q_i(t)$ and $\overline{q^*}$ are the adsorption capacity at time t and at the equilibrium absorption time, respectively. k_f, k_e, k_s, k_A and k are the rate constants of the pseudo-first order, Elovich, pseudo-second order, Avrami and Fractional order, respectively. m_e denotes initial adsorption rate of Elovich equation, and m the fractional order equation constant. n and n_A reflect the reaction of pseudo-order and Fractional order with respect to a driving force, respectively. According to the TGA experiment in Section 3.2, the kinetic parameters of TC-5A and PSA-5A can be inferred as shown in Table 4 when C_{CO_2} = 0.75%.In order to predict the accuracy of kinetic equations, the average absolute percentage deviation E is adopted as shown in:

$$E = \frac{\sum_{i=1}^{N}(q_{\exp,i} - q_{\text{sim}})/q_{\exp,i}}{N} \times 100\% \quad (1)$$

where $q_{\exp}$ and q_{sim} are the adsorption capacity in experimental and simulation condition, respectively; N is the total number of experiments.

The errors of adsorption kinetic equations are listed in Table 5.

There exist obvious differences among these equations. Some have remarkable high error, such as the pseudo-first order, Elovich and the pseudo-second order equation. Their E values in Table 5 are all over 10%. But for the Avrami's equation and the Fractional order kinetic equation, their maximum E value is lower than 5%. Furthermore, the Avrami's equation uses less number of kinetic parameters than the fractional order equation, and it has distinctly lower error values.

Table 3 Different adsorption kinetic equations.

Kinetic equation	Differential form	Equation
Pseudo-first order	$\frac{\partial q_i}{\partial t} = k_f(\overline{q^*} - q_i)$	$q_i(t) = \overline{q^*}(1 - e^{-k_f t})$
Elovich	$\frac{\partial q_i}{\partial t} = k_e e^{-m_e q_i}$	$q_i(t) = \frac{2.3}{m_e}\left[lg\left(t + \frac{1}{k_e m_e}\right) + lg(k_e m_e)\right]$
Pseudo-second order	$\frac{\partial q_i}{\partial t} = k_s(\overline{q^*} - q_i)^2$	$q_i(t) = \frac{q^* t}{1/(k_s q^*) + t}$
Avrami	$\frac{\partial q_i}{\partial t} = k_A^{n_A} t^{n_A - 1}(\overline{q^*} - q_i)$	$q_i(t) = \overline{q^*}[1 - \exp(-kt)^{n_A})]$
Fractional order	$\frac{\partial q_i}{\partial t} = k t^{m-1}(\overline{q^*} - q_i)^n$	$q_i(t) = \overline{q^*} - 1 \Big/ \left[\left(\frac{(n-1)k}{m}\right)t^m + \left(\frac{1}{q^*}\right)^{n-1}\right]^{1/(n-1)}$

Table 4 Kinetic equation parameter values.

Parameter	TC-5A (298 K)	PSA-5A (323 K)
k_f	0.0021	0.00247
k_e	1.1892×10^{-5}	1.2×10^{-6}
m_e	262.0698	50.0064
k_s	0.0588	0.612
k_A	0.001	0.0015
n_A	1.2	1.22
k	0.0001	0.0002
m	1.2045	1.5851
n	0.7461	1.1908

Table 5 Kinetic equation errors.

Kinetic equation	E for TC-5A (%)	E for PSA-5A (%)
Pseudo-first order	29.6666	25.3289
Elovich	12.9859	25.2348
Pseudo-second order	22.001	25.2810
Avrami	1.8625	3.9875
Fractional order	3.3494	7.2181

Hence we suggest adopting the Avrami's equation to describe the adsorption process for TC-5A and PSA-5A.

4. Experimental study of CO_2 adsorption in packed bed column

In the industrial researches, the experimental conditions were usually kept at high initial CO_2 concentration or high temperature adsorption to verify the adsorbents' performance.[8,13,15,17–20] Many of them even considered the effect of trace contaminants or volatile organic compounds (VOC). While in our aerospace investigation, we probably consider the experimental condition at room temperature and low CO_2 concentration with water vapor.

In Section 3, the TGA experiments help us to understand the single particles adsorption performance for TC-5A and PSA-5A, and the adsorption performances in a packed bed column still need to be verified. In this section, the packed bed column experiment is set up. The experiments involve the dry air and the moist air with different RH, the inlet CO_2 concentration is kept at less than 1.0% in volume at fixed temperature, and the temperature effect is also considered in dry air and moist air experiments.

4.1. Experimental setup

Fig. 6 shows the experimental flow diagram of CO_2 adsorption experiments in a packed bed column. A stainless steel column (with 0.2 cm inner diameter and 20 cm packed height) is filled with TC-5A or PSA-5A at atmospheric pressure. The flow rate is 1.5 L/min controlled by the mass flow-meter. The pure N_2 is humidified by a moistener to realize different RH in feed air, as well as the RH values at the entrance and exit port displayed through the temperature and humidity recorder. The K-type thermocouple is placed in the middle of inner bed to monitor the material temperature when adsorbing, while the other one measured the room temperature. The outlet CO_2 concentration is obtained using the IRA, in front of which a drying tube (filled with the silica gels) is installed to remove water vapor. The packed bed column is equipped with the direct-current power supply which is used for heating when necessary. All the data in testing equipment is uploaded to the computer and the apparatuses are shown in Fig. 7.

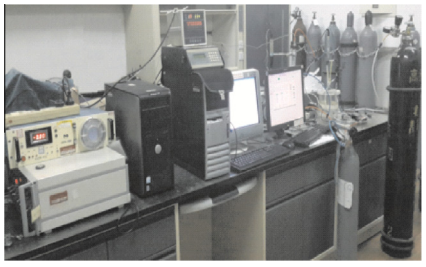

Fig. 7 Apparatuses photo of packed bed column experiment.

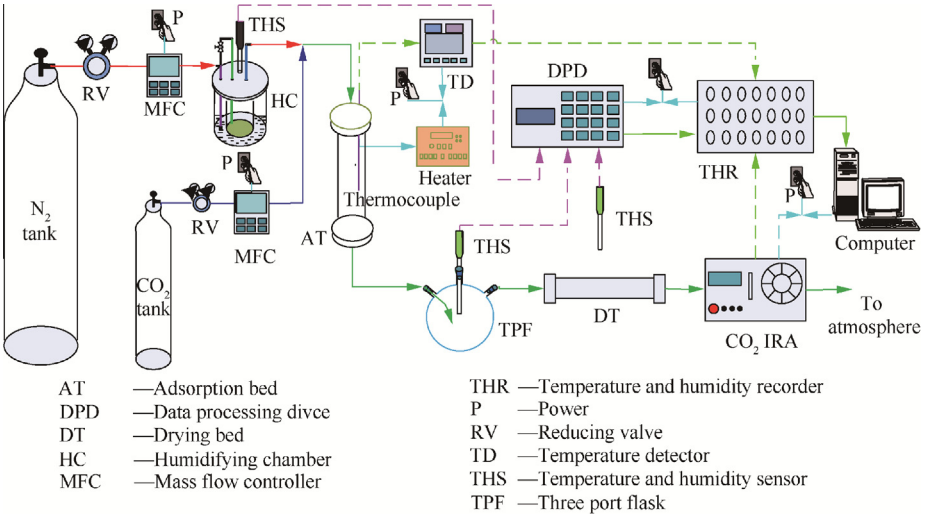

Fig. 6 Experimental flow diagram of packed bed column.

4.2. CO_2 adsorption performance analysis for drying air

4.2.1. Experiments at 298 K

In this section, we focus on investigating the impact of CO_2 concentration in dry feed air on the adsorption performance of TC-5A and PSA-5A at 298 K. The investigated CO_2 concentrations include 0.5%, 0.75% and 1.0%. The experimental results of CO_2 outlet concentration are shown in Fig. 8. From Fig. 8, we can draw the following conclusions:

(1) TC-5A breakthrough time decreases with increasing initial CO_2 concentration. It takes about 20 min to break when C_{CO_2} = 0.5% and it decreases to 5 min when C_{CO_2} = 1.0%.
(2) PSA-5A breakthrough time is about 23 min when C_{CO_2} = 0.7%.
(3) The CO_2 adsorption performance of PSA-5A is better than the one of TC-5A under the same condition. The reason might be that PSA-5A has a smaller diameter particle and larger porosity than TC-5A, which benefits the adsorption under the same condition.

4.2.2. Experiments at 323 K

In the following experiments, the adsorbent temperature is controlled by the direct-current power supply. The CO_2 breakthrough curves at 323 K are shown in Fig. 9 when C_{CO_2} = 0.7%.

From Fig. 9, CO_2 penetrates the TC-5A bed column after 3 min and rises rapidly to the equilibrium at 323 K. The adsorption time significantly reduced at 323 K compared to the one at 298 K. Simultaneously, the adsorption time of PSA-5A in packed bed column is also shortened from 25 min at 298 K to 10 min at 323 K, but its adsorption capacity still shows better than the one of TC-5A.

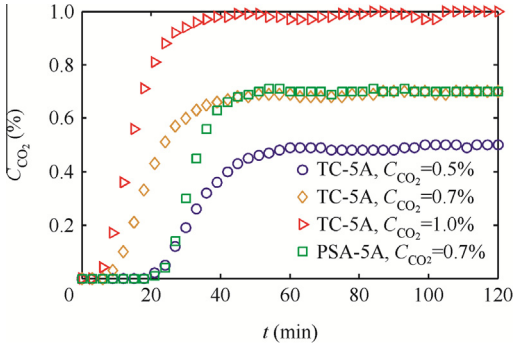

Fig. 8 CO_2 breakthrough curves for TC-5A and PSA-5A at 298 K.

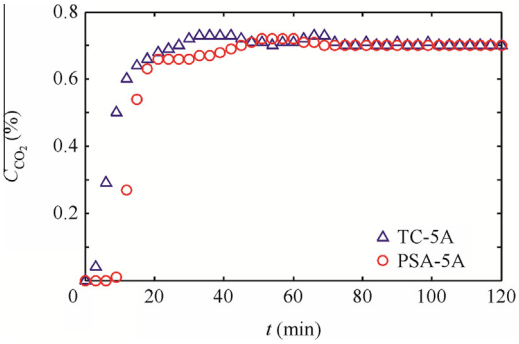

Fig. 9 CO_2 breakthrough curves for TC-5A and PSA-5A at 323 K.

4.3. CO_2 adsorption performance with different RH

The molecular sieve has stronger adsorption ability for water vapor than CO_2. In order to investigate the CO_2 adsorption performance under different RH conditions, we conduct the following experiments.

4.3.1. Experiments at 298 K

In all these experiments, the absorption temperature is controlled at 298 K.

For TC-5A, the experimental conditions are C_{CO_2} = 0.7%, and RH = 20%, 40% and 60%, respectively. While for PSA-5A, the experimental conditions are C_{CO_2} = 0.7% and RH = 40%. The experimental results are shown in Fig. 10.

In these experiments, water vapor data kept 0 all the experimental time for the two molecular sieves, so the outlet RH is not shown in Fig. 10. The experimental results reveal the following conclusions:

(1) We compare the experimental results of TC-5A and PSA-5A in Figs. 8 and 10, and find that the CO_2 breakthrough time is shortened.
(2) Vapor has a tremendous influence on the CO_2 adsorption especially when RH is beyond 20%.
(3) The CO_2 concentration in Fig. 10 presents a fluctuation phenomenon after the adsorption reaches its dynamic equilibrium. This can be attributed to the exothermic heat accumulation in fixed bed column that affects the equilibrium adsorption characteristic.

4.3.2. Experiments at 323 K

We heated the temperature of the packed bed column to 323 K and the other conditions are the same as Fig. 10. The new experimental results are shown in Fig. 11. Fig. 11 indicates that:

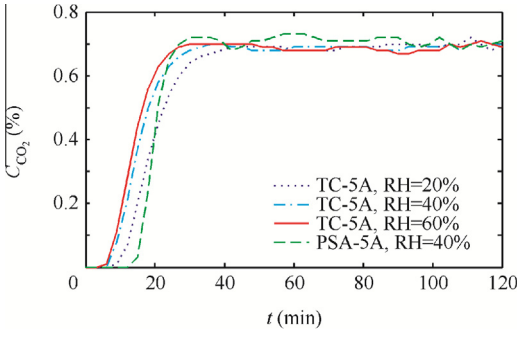

Fig. 10 CO_2 breakthrough curves with different RH at 298 K.

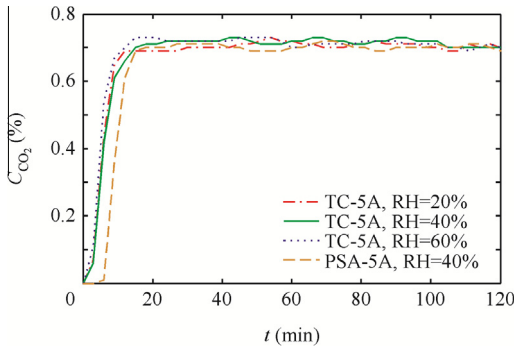

Fig. 11 CO_2 breakthrough curves with different RH at 323 K.

(1) The CO_2 breakthrough time of TC-5A at 323 K is slightly shortened with the increasing RH compared to the one at 298 K.
(2) It takes a longer adsorption time for PSA-5A than the one of TC-5A, but the PSA-5A adsorption time at 323 K is still less than the one at 298 K.
(3) Although the RH is a key factor for CO_2 adsorption, the temperature cannot be neglected.

5. Mathematical model and dynamic analysis

Fixed bed is an important unit for the 4-BMS subsystem in a manned spacecraft. For a fixed bed design, it is valuable to set up a proper mathematical model to analyze its dynamic performance. In this section, we will discuss this model and its precision.

Some adsorption mathematical models in fixed-bed column have been developed and most of them use the LDF equation to approximately describe the gas–solid mass transfer mechanism.[1] In Section 3.3, we draw a conclusion that the Avrami's equation has more accurate than LDF equation. Therefore, we will introduce a new model with Avrami's equation.

In the following analysis, some principal assumptions are used[28,35]:

(1) The adsorption process is isothermal and it can be described by the Henry isotherm model.
(2) The velocity in the bed column is not changed by the adsorbent and heat effect.
(3) There are no radial variations for temperature, pressure and concentration in the solid and the gas phase.
(4) Heat and mass transfer is instantaneous and the plug flow is assumed with no axial or radial dispersion.
(5) The gas phase follows the ideal gas law.

With these assumptions, the concentration change rate at any axial position along the column is given by:

$$-D_{zi}\frac{\partial^2 C_i}{\partial z^2}+\frac{\partial}{\partial z}(uC_i)+\frac{\partial C_i}{\partial t}+\frac{1-\varepsilon_b}{\varepsilon_b}\rho_p\frac{\partial \overline{q_i}}{\partial t}=0 \tag{2}$$

where D_{zi} is axial diffusion coefficient, m^2/s; C_i represents the adsorbate concentration in the gas phase, kg/m^3; u is the fluid velocity, m/s; z is the distance along the packed bed length, m; t is time, s; $\overline{q_i}$ indicates the average adsorption of component i, kg/m^3.

Assuming that adsorbents are homogeneous spherical particles, the intra-particle mass transfer is described by the Fick diffusion law as[36]:

$$\frac{\partial \overline{q_i}}{\partial t}=D_e\left(\frac{\partial^2 C_i}{\partial r^2}+\frac{2}{r}\cdot\frac{\partial C_i}{\partial r}\right)=D_e\left(\frac{\partial}{\partial r}\left(r^2\frac{\partial C_i}{\partial r}\right)\right) \tag{3}$$

where D_e is effective diffusion in particles, m^2/s; r the distances along the radius of particles, m. The adsorption capacity, q_i, forms a link between the gas-phase and solid-phase mass balance equations. The effects of all the mechanisms can be lumped into a single effective axial dispersion coefficient. Because the Avrami's equation has more accuracy than LDF equation, we will use the Avrami's equation to calculate the average adsorption capacity.

$$\frac{\partial \overline{q_i}}{\partial t}=k_A^n t^{n-1}(\overline{q^*}-\overline{q_i}) \tag{4}$$

The axial diffusion coefficient D_{zi} can be estimated using the following correlation:

$$\frac{\varepsilon_b D_{zi}}{D_{mi}}=20+0.5ScRe \tag{5}$$

where D_{mi} is the molecular diffusivity of component i, m^2/s; Sc and Re are the Schmidt and Reynolds number, respectively.

The molecular diffusion of component i is estimated by the Chapman–Enskog equation under low partial pressure conditions[31,37,38]:

$$D_{mi}=\frac{0.001858T^2\left(\frac{1}{M_A}+\frac{1}{M_B}\right)^{1/2}}{P\delta_{AB}^2\Omega(\varepsilon/KT)} \tag{6}$$

where δ_{AB} is diameter for molecular collision, m; M_A and M_B are the molecular weight for two components, kg; P is the atmospheric pressure, Pa; Ω the Lennard–Jones collision integral function and it is connected with the temperature ratio ε/KT; K the Boltzmann constant, J/K; ε the potential energy of molecular interaction; δ_{AB} and ε/KT can be obtained in Refs.[38–40]

The following initial conditions are imposed:

$$\overline{q}_i|_{t=0}=0;\ C_i|_{z=0}=C_0,\ t\geqslant 0$$

The boundary condition is

$$\left.\frac{\partial C_i}{\partial z}\right|_{z=L}=0;\ t\geqslant 0$$

where L is the length of packed bed column. Eqs. (2)–(6) form the gaseous mass transfer correlations in the adsorption bed column. Here we name it as the new Avrami's model.

These correlations contain the coupled partial differential equations (PDEs) and can be solved by the finite difference technique conveniently. The PDEs are discretized by the first-order upwind or second-order differences in time and spatial dimensions.

Different simulation cases will be designed based on the experimental conditions of C_{CO_2} = 0.7%. Two experiments are used to inspect the accuracy of the established dynamic models. Physical parameters of molecular sieve can be seen in Table 4 in Section 3.3. The simulation conditions and the related parameters are listed in Tables 6 and 7, respectively. In Table 7, R_p is the mean radius for molecular sieve particles, D is the diameter of packed bed column.

Table 6 Operating and simulation conditions in fixed bed adsorption experiments.

No.	T (K)	Case	Model	Adsorbent
1	298	1-1	LDF	TC-5A
1	298	1-2	Avrami	TC-5A
2	323	2-1	LDF	PSA-5A
2	323	2-2	Avrami	PSA-5A

Table 7 Parameters in different simulation cases.

Case	D_{zi} (10^{-6} m^2/s)	D_{mi} (10^{-8} m^2/s)	R_p (mm)	L (m)	D (m)	u (m/s)
1-1	1.250	1.07	1.000	0.045	0.02	0.08
1-2	0.963	1.07	1.000	0.045	0.02	0.08
2-1	1.590	1.13	0.375	0.035	0.02	0.08
2-2	1.590	1.13	0.375	0.035	0.02	0.08

(1) Simulation comparison for Experiment 1.

The simulation curves are obtained using the classic LDF model and the new Avrami's model, respectively. Fig. 12 gives the CO_2 concentration breakthrough curves for TC-5A. The simulation result of the new Avrami's model in Fig. 12 is relatively closer to the experimental results than the LDF model.

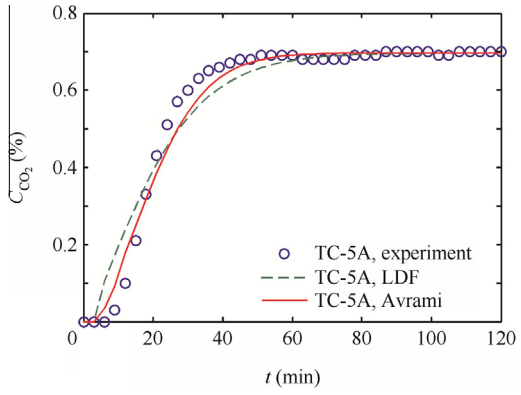

Fig. 12 Comparison results of Experiment 1 (C_{CO_2} = 0.7%, 298 K).

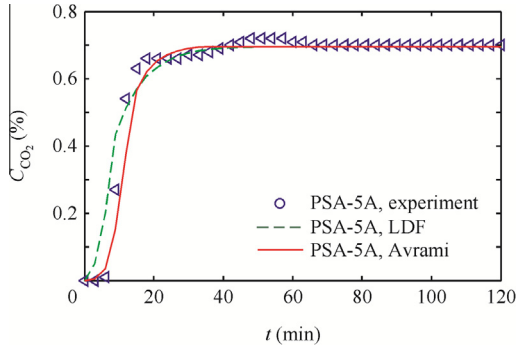

Fig. 13 Comparison results of Experiment 2 (C_{CO_2} = 0.7%, 323 K).

(2) Simulation comparison for Experiment 2.

The simulation results are compared for PSA-5A as shown in Fig. 13. The simulating curves of PSA-5A are in accordance with the most experimental data at 323 K. The simulation error of the classic LDF is larger than the one of the Avrami's model.

6. Conclusions

Two kinds of molecular sieve materials, TC-5A and PSA-5A, were produced and tested. The TGA experiments and the packed bed column experiments were established to test the adsorbing performance under different conditions. The experimental conditions are determined according to the studied confined space, thus the room temperature, low CO_2 concentration and different RHs with 20% to 60% are used in our study. Besides, the kinetic equation for TC-5A and PSA-5A is analyzed carefully according to the experimental results. We compare the accuracy of different mass transfer dynamic models and replace the LDF model with the new Avrami's model. Results are as follows.

(1) According to the TGA experiments and the packed bed column experiments, the results demonstrate the good adsorption performance at low CO_2 concentration and room temperature, which is obviously different from the industrial adsorbents.
(2) The impact of concentration changes on adsorption is obvious when $C_{CO_2} \leqslant 1.0\%$ in volume. From the TGA experimental results, the concentration increases from 0.5% to 1.0%, and the corresponding CO_2 loading in adsorbents will be doubled. Furthermore, the relationship of the equilibrium adsorption and the initial CO_2 concentration basically follows the Henry's law when temperature is given. Nevertheless, the adsorption capacity will be decreased by 80% approximately when the adsorption temperature reaches 323 K. The verified reasonable adsorbing temperature range is 283–303 K.
(3) Five kinetic equations are discussed. Compared to the experimental data, the Avrami's equation is the best fit by calculating the average absolute percentage deviation and it can reflect the complicated mechanism for TC-5A and PSA-5A particles.
(4) The packed bed column adsorption experiments also demonstrate that the concentration and temperature of feed air strongly influence the equilibrium adsorption. In addition, the adsorption capacity value decreases to 3.64% compared to the one in TGA experiment.
(5) Water vapor experiments in the packed bed show that the materials belong to the hydrotropic substance and have powerful capability of H_2O adsorption due to the strong polar. CO_2 adsorption will be greatly affected if the water vapor exists in air, and the influence of water vapor on the CO_2 adsorption performance cannot be neglected.

(6) The adsorption process of TC-5A and PSA-5A in packed bed column can be predicted by the established dynamic models. The improved model, named the new Avrami's model, is considered based on the Avrami's equation. Results reveal that both models can predict the mass transfer process for TC-5A and PSA-5A, but the new Avrami's model has more accuracy than the classic LDF model.

(7) The experiments and simulation studied in this paper is helpful for the 4-BMS subsystem design and can provide some technical support for the development of manned spaceflight in China.

Acknowledgments

The authors gratefully acknowledge the financial support of the Open Funding Project of National Key Laboratory of Human Factors Engineering (No. SYFD14005181K).

References

1. Shafeeyan MS, Daud WMAW, Shamiri A. A review of mathematical modeling of fixed-bed columns for carbon dioxide adsorption. *Chem Eng Res* 2014;**92**(5):961–88.
2. Liu Y, Ye Q, Shen M, Shi J, Chen J, Pan H, et al. Carbon dioxide capture by functionalized solid amine sorbents with simulated flue gas conditions. *Environ Sci Technol* 2011;**45**(13):5710–6 [Chinese].
3. Jones HW. Carbon dioxide reduction system trade studies. *Proceedings of the 41st international conference on environmental systems*. Reston: AIAA; 2011.
4. Wang K, Gao F. Review and prospects of fifty years' development of environment control and life support system in manned spacecraft. *Space Med Med Eng* 2012;**24**(6):435–43 [Chinese].
5. Carrasquillo RL. ISS ECLSS technology evolution for exploration. *Proceedings of the 43rd AIAA aerospace sciences meeting and exhibit*. Reston: AIAA; 2005.
6. MacCallum T, Finger B. The next generation of ECLSS: life support outside the Earth–Moon system. *AIAA SPACE 2013 conferences & AMP*. Reston: AIAA; 2013.
7. Anderson M, Rotter H, Stambaugh I, Yagoda E. Life support systems for a new lunar lander. *Proceedings of the 42nd international conference on environmental systems*. Reston: AIAA; 2012.
8. Zhou JH, Zhao HL, Zhu YJ, Hu J, Liu HL, Hu Y. Molecular simulation modeling study of CO_2 adsorption and separation for 5A-MCM-41 microporous/mesoporous composite materials. *Proceedings of the 17th Chinese zeolite conference (17 CZC)*. Beijing: Chinese Chemical Society; 2013 [Chinese].
9. Gai WD, Wang HL. Closed-loop dynamic control allocation for aircraft with multiple actuators. *Chin J Aeronaut* 2013;**26**(3):676–86.
10. Sun HB, Li SH. Composite control method for stabilizing spacecraft attitude in terms of Rodrigues parameters. *Chin J Aeronaut* 2013;**26**(3):687–96.
11. Chen ZH, Du FZ, Tang XQ. Research on uncertainty in measurement assisted alignment in aircraft assembly. *Chin J Aeronaut* 2013;**26**(6):1568–76.
12. Pahl C, Pasel C, Luckas M, Bathen D. Adsorptive water removal from primary alcohols and acetic acid esters in the ppm-region. *J Chem Eng Data* 2012;**57**(9):2465–71.
13. Liang H, Gao H, Kong Q, Chen Z. Adsorption equilibrium and kinetics of tetrahydrofuran + water solution mixture on zeolite 4A. *J Chem Eng Data* 2006;**51**(1):119–22.
14. Liang H, Gao H, Kong Q, Chen Z. Adsorption of tetrahydrofuran + water solution mixtures by zeolite 4A in a fixed bed. *J Chem Eng Data* 2007;**52**(3):695–8.
15. Silvestre-Albero AM, Wahby A, Silvestre-Albero J, Rodriguez-Reinoso F, Betz W. Carbon molecular sieves prepared from polymeric precursors: porous structure and hydrogen adsorption properties. *Ind Eng Chem Res* 2009;**48**(15):7125–31.
16. Hossein Z, Hejazi SA, Avila AM, Kuznicki TM, Wei Z, AKuznicki SM. Characterization of natural zeolite membranes for H_2/CO_2 separations by single gas permeation. *Ind Eng Chem Res* 2011;**50**(22):12717–26.
17. Wang D, Ma X, Sentorun-Shalaby C, Song C. Development of carbon-based "molecular basket" sorbent for CO_2 capture. *Ind Eng Chem Res* 2012;**51**(7):3048–57.
18. Lively RP, Chance RR, Kelley BT, Deckman HW, Drese JH, Jones CW, et al. Hollow fiber adsorbents for CO_2 removal from flue gas. *Ind Eng Chem Res* 2009;**48**(15):7314–24.
19. Opembe NN, Guild C, King Ondu C, Nelson NC, Slowing II, Suib SL, et al. Vapor-phase oxidation of benzyl alcohol using manganese oxide octahedral molecular sieves (OMS-2). *Ind Eng Chem Res* 2014;**53**(49):19044–51.
20. Guo B, Hong L, Jiang H. Macroporous poly (calcium acrylate-divinylbenzene) bead A selective orthophosphite sorbent. *Ind Eng Chem Res* 2003;**42**(22):5559–67.
21. Yuh-Shan H. Citation review of Lagergren kinetic rate equation on adsorption reactions. *Scientometrics* 2004;**59**(1):171–7.
22. Ayoob S, Gupta AK, Bhakat PB, Bhat VT. Investigations on the kinetics and mechanisms of sorptive removal of fluoride from water using alumina cement granules. *Chem Eng J* 2008;**140**(1):6–14.
23. Heydari-Gorji A, Sayari A. CO_2 capture on polyethylenimine-impregnated hydrophobic mesoporous silica: experimental and kinetic modeling. *Chem Eng J* 2011;**173**(1):72–9.
24. Nalette T, Reiss J, Filburn T, Mahan E, Seery T, Weiss B, et al. Development of an amine-based system for combined carbon dioxide, humidity, and trace contaminant control. *Proceedings of the 35th international conference on environmental systems*. Washington, D.C.: NASA; 2005.
25. Tran TH, Govin A, Guyonnet R, Grosseau P, Lors C, Damidot D, et al. Avrami's law based kinetic modeling of colonization of mortar surface by alga Klebsormidium flaccidum. *Int Biodeter Biodegr* 2013;**79**(1):73–80.
26. Lopes EC, Dos Anjos FS, Vieira EF, Cestari AR. An alternative Avrami equation to evaluate kinetic parameters of the interaction of Hg (II) with thin chitosan membranes. *J Colloid Interface Sci* 2003;**263**(2):542–7.
27. Serna-Guerrero R, Sayari A. Modeling adsorption of CO_2 on amine-functionalized mesoporous silica. 2: kinetics and breakthrough curves. *Chem Eng J* 2010;**161**(1):182–90.
28. Gray ML, Hoffman JS, Hreha DC, Fauth DJ, Hedges SW, Champagne KJ, et al. Parametric study of solid amine sorbents for the capture of carbon dioxide. *Energy Fuel* 2009;**23**(10):4840–4.
29. Farooq S, Huang QL, Karimi IA. Identification of transport mechanism in adsorbent micropores from column dynamics. *Ind Eng Chem Res* 2002;**41**(5):1098–106.
30. Ostroski IC, Borba CE, Silva EA, Arroyo PA, Guirardello R, Barros MA. Mass transfer mechanism of ion exchange in fixed bed columns. *J Chem Eng Data* 2011;**56**(3):375–82.
31. Welty JR, Wicks CE, Rorrer G, Wilson RE. *Fundamentals of momentum, heat, and mass transfer*. New York: John Wiley & Sons; 2009.
32. Mohamadinejad H. *The adsorption of $CO_2/H_2O/N_2$ on 5A zeolite and silica gel in a packed column in one and two-dimensional flows* [dissertation]. Huntsville: University of Alabama; 1999.
33. Liu JQ. *Separation process and simulation*. Beijing: Tsinghua University Press; 2007. p. 330–9 [Chinese].
34. Mulgundmath VP, Jones RA, Tezel FH, Thibault J. Fixed bed adsorption for the removal of carbon dioxide from nitrogen: breakthrough behaviour and modelling for heat and mass transfer. *Sep Purif Technol* 2012;**85**(1):17–27.
35. Bard AJ, Faulkner LR. *Adsorbents fundamentals and applications*. 2nd ed. New York: Wiley; 2001. p. 55–64.

36. Qian XS. *Physical and mechanical notes*. Beijing: Science Press; 1962. p. 309–17 [Chinese].
37. Ruthven DM. *Principles of adsorption and adsorption processes*. Hoboken: John Wiley & Sons; 1984. p. 173–97.
38. Lu NX. *Chemical unit operation manual (a)—the basis of chemical calculation data*. Xi'an: The Sixth Design Institute of the Ministry of Chemical Industry; 1966. p. 113–5 [Chinese].
39. Reid RC, Prausnitz JM, Poling BE. *The properties of gases and liquids*. 5th ed. New York: McGRAW-HILL; 2001. p. 11-3–11-19.
40. Li RQ. Empirical formula of calculating gas transfer coefficient of the Lennard–Jones molecular collision function. *Chem Eng* 1974;**6** (1):1–3 [Chinese].

Liu Meng received the B.S. and Ph.D. degrees in School of Aeronautic Science and Engineering from Beihang University in 1996 and 2003, respectively, then continued to be the post-doctorate there and became a teacher in Beihang University. His main research interests are mainly engaged in the limited space environment control and simulation research.

Yang Dongsheng is a M.D.-Ph.D. student at School of Aeronautic Science and Engineering, Beihang University. His area of research includes the air regeneration technology research of manned spacecraft.

Pang Liping is a professor and Ph.D. supervisor at School of Aeronautic Science and Engineering, Beihang University. She received the Ph.D. degree and completed her postdoctoral research from the same university in 2002 and 2007, respectively. She has published more than 30 papers. Her current research interests are aircraft integrated environmental control and environmental simulation.

Yu Qingni is an associate professor at National Key Laboratory of Human Factors Engineering of China Astronaut Research and Training Center. She received the B.S. degree at the Department of Earth and Space Science from the University of Science and Technology of China in 1993. She presided over or participated in the design from 1st to 8th of the Shenzhou spacecraft and her research area is atmospheric purification technology in manned spacecraft.

Huang Yong is a full professor at Beihang University. He received his Ph.D. degree in engineering thermophysics from Harbin Institute of Technology in 2003. He completed his postdoctoral research on engineering mechanics in Tsinghua University in 2005. He has published more than 60 papers. His primary research interests include thermal radiation transfer of graded index medium, microscale thermal radiation as well as infrared transmission modeling and analysis.